Macromolecular Chemistry and Physics
www.mcp-journal.de

Small-Angle X-Ray Scattering Measurements on Amphiphilic Polymer Conetworks Swollen in Orthogonal Solvents

*Lena Benski, Ismail Viran, Frank Katzenberg, and Joerg C. Tiller**

Amphiphilic polymer conetworks (APCNs), which combine two different polymer nanophases, have a broad range of applications that involve their unique potential to separately swell one of these nanophases in a selective solvent. Little is known about the structural changes of such APCNs upon swelling in dependence on the topology. Here, conetworks composed of poly(2-ethylhexyl acrylate) crosslinked by poly(2-methyl-2-oxazoline) (PMOx) are investigated with small-angle X-ray scattering in dry and swollen state using the orthogonal solvents water and toluene. The data clearly show that the structural changes induced by swelling are strongly dependent on the topology of the APCNs. While water leads to fusion of PMOx phases resulting in larger structures than found in the dry APCN, toluene is only swelling the hydrophobic phases without structural changes.

1. Introduction

Amphiphilic polymer conetworks (APCNs) are versatile nanomaterials that can combine seemingly incompatible properties. They are composed of two different, immiscible polymers that are crosslinked with each other, which lead to the formation of nanostructures by nanophase separation. Therefore, APCNs are able to swell in both hydrophilic and hydrophobic solvents.[1] This outstanding characteristic enables them for numerous applications. The most eminent use of APCNs is soft contact lenses.[2] Besides this commercial application, APCNs may function as carriers for drug delivery such as tubular networks for insulin delivery.[3] They can also be employed as matrix for orthopedic tissue engineering[4] and antimicrobial coatings.[5] Another area of applications is optical chemical and biomedical sensors for peroxide detection.[6] They can also be used as membranes with pH[7] and thermally responsive swelling[7e,8] as well as for chiral separation,[9] and even APCNs with controlled ion conductivity[10] and self-healing properties have been reported.[11] Another important field of APCNs is their use as activating carriers for enzymes.[12] For example, Bruns et al. reported that their use could enhance the activity of enzymes in supercritical CO_2.[13] APCNs also have been shown to activate enzymes such as lipase in organic media.[14] Sittko et al. stated that this enhancement of the enzyme activity derives from the nanostructure of the networks.[14a] According to Kennedy et al. the key characteristics of APCNs are the coexistence of a hydrophilic and a hydrophobic phase that are covalently crosslinked and the presence of phase cocontinuity.[1a]

The synthesis of APCNs also nicely summarized by Kennedy follows varying strategies that lead to different network topologies. The macromonomer crosslinker approach results in topologies where one phase is most likely always connected while the other is isolated.[15] The crosslinking approach of block copolymers and star polymers leads to a connected and an unconnected phase with defined distances from the crosslinking points.[16] Crosslinking of different homopolymers are more homogeneously connected.[17] In all cases, the amphiphilic nature of the polymer segments results in a mostly cocontinuous nanophase separation that leads to a distinguished nanostructure, which is more or less similar in all cases. Swelling of these structures is usually presumed to be depending on this nanostructure with the only difference that the T_g of the polymers is influencing the degree of swelling. The influence of the network topology on the swelling behavior is rarely considered.

The nanostructure of the APCNs, which often consists of cocontinuous phases but can also consist of spherical/spheroidal and lamellar morphologies, has been widely characterized, using atomic force microscopy (AFM),[17a,18] transmission electron microscopy (TEM),[19] and solid-state NMR[20] amongst others. However, these methods usually only allow the characterization of the samples in the dry state. AFM can be also used to characterize APCNs in swollen state, but the method can only detect the structure at the surface of the sample, which is swelling differently than the bulk because it has less constrains. This limitation can be overcome by using scattering techniques such as small-angle X-ray scattering (SAXS) and small-angle neutron scattering

L. Benski, I. Viran, Dr. F. Katzenberg, Prof. J. C. Tiller
Biomaterials and Polymer Science
Department of Bio- and Chemical Engineering
TU Dortmund
Emil-Figge-Straße 66, Dortmund 44227, Germany
E-mail: joerg.tiller@tu-dortmund.de

The ORCID identification number(s) for the author(s) of this article can be found under https://doi.org/10.1002/macp.202000292.

DOI: 10.1002/macp.202000292

(SANS). Hoffmann et al. used SANS measurements to analyze interconnected amphiphilic "in–out" star copolymers swollen in water.[21] They reported a correlation between the degree of order of the structure of the networks and their macroscopic elasticity. Hayward et al., Spiess et al., and Boesel et al. amongst others used SAXS to identify the structure of the nanophases of dry APCNs.[20a,22] Grossmann et al. used SAXS in order to investigate the water uptake of hydrogels based on poly(ethylene oxide).[23] Papadakis et al. studied water-swollen crosslinked amphiphilic block copolymers consisting of a hydrophobic block based on 2-ethylhexyl methacrylate or lauryl methacrylate surrounded by a hydrophilic block from 2-(dimethylamino)ethyl methacrylate using SAXS.[24] They reported strong microphase separation for the networks and model fitting revealed that the networks consist of densely packed hydrophobic cores, which are surrounded by the swollen hydrophilic polymer. These findings coincide with the star-like structure of the block copolymers used for the networks. Shibayama et al. used SAXS to analyze the structure of poly(ethylene glycol)–poly(dimethylsiloxane) amphiphilic conetwork gels.[25] When they substituted the solvent with methanol and water, a microphase separation occurred and the macroscopic size of the networks decreased. Kennedy et al. studied APCNs containing polyisobutylene and poly(2-hydroxyethyl methacrylate) and poly(*N*,*N*-dimethylacrylamide), respectively, with various compositions.[26] SAXS measurements of the dry networks confirmed interdomain spacings of 6–17 nm. When the acrylamide containing networks were swollen in heptane their domain size increased by a factor of up to 1.3. However, these networks could not be analyzed in water because of insufficient electron density difference between the different components. The networks containing the methacrylate on the other hand exhibited a maximum increase of the domain size by a factor of 1.2 when swollen in heptane and 1.02 when swollen in water.

However, none of these studies showed any signs of the influence of the network topology on the swelling behavior of both phases. In order to address this for the first time, we used the potential of SAXS for analyzing domains in APCNs in their swollen state. The study is based on an APCN prepared by the macromolecular crosslinker approach, which should provide a continuous polymer phase prepared by the free radically polymerized hydrophobic 2-ethylhexyl acrylate (EhAc) and a partially isolated poly(2-methyl-2-oxazoline) (PMOx) phase which was used as hydrophilic crosslinker. The study addresses the swelling of both phases by a respective selective solvent and their structural change followed by SAXS.

2. Results and Discussion

APCNs based on methacrylamide terminated PMOx as crosslinker and poly(2-ethylhexyl acrylate) (PEhAc) as linear polymer have been reported to significantly enhance the enzyme activity of entrapped lipase Cal B in the organic media heptane and toluene by a factor of some 20 compared to the suspended enzyme powder in the respective organic solvents.[14a] Sittko et al. stated that this activation originates from the nanostructure of these amphiphilic networks. However, the structural change of the swelling of the nanophases is not fully understood so far. The aim of this study was to gain a better insight into the structure of the nanophases of APCNs swollen in a solvent that is selective to one phase. To this end, APCNs based on hydrophilic PMOx (30 repeating units) acting as the crosslinker and hydrophobic EhAc acting as the polymer phase were prepared according to Sittko et al.[14a] (see **Figure 1**) and analyzed using SAXS in order to gain information on the swollen state of the nanophases in water and toluene.

APCNs with 30–100 wt% PMOx (PEhAc-*l*-PMOx(30) to *x*-PMOx(100)) were prepared this way. All networks were optically clear indicating absence of macrophase separation in all cases. After extraction with chloroform, a sol content of less than 25 wt% was found in all cases (see **Table 1**) and the composition did not change significantly according to FTIR measurements (see Table S1 and Figure S3, Supporting Information).

In order to analyze the structure of the nanophases in the swollen state, first, the degree of swelling *S* was gravimetrically determined for the networks used in this study (see **Figure 2**). S_{water} expectedly increases with increasing amount of the hydrophilic PMOx from 1.6 for PEhAc-*l*-PMOx(30) to 6.8 for *x*-PMOx(100). $S_{toluene}$ decreases from $S_{toluene}$ = 4.6 for the network with 30 wt% PMOx to 1.0 for the networks with

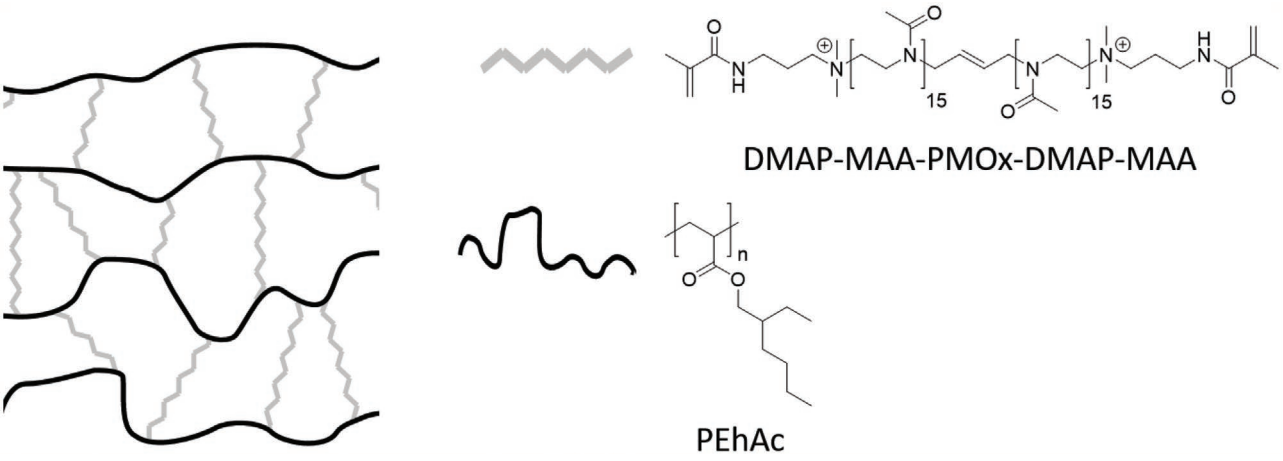

Figure 1. Schematic overview of the prepared APCNs with the hydrophilic *N*-[3-(dimethylamino)-propyl]-methacrylamide (DMAP-MAA) terminated poly(2-methyl-2-oxazoline) (PMOx) acting as macro-crosslinker and the hydrophobic poly(2-ethylhexyl acrylate) (PEhAc) acting as polymer phase.

Table 1. Overview of the reactions mixture of the PEhAc-*l*-PMOx conetworks, their composition, and gel content after extraction in chloroform.

APCN	PMOx [mg]	EhAc [mg]	1M2P [µL]	PMOx [wt%]	Gel content [wt%]
PEhAc-*l*-PMOx(30)	61.25	157.30	220	30	81
PEhAc-*l*-PMOx(50)	60.07	67.41	150	50	76
PEhAc-*l*-PMOx(70)	61.01	29.21	140	70	81
PEhAc-*l*-PMOx(90)	54.57	6.74	70	90	82
x-PMOx(100)	59.10	0	80	100	96

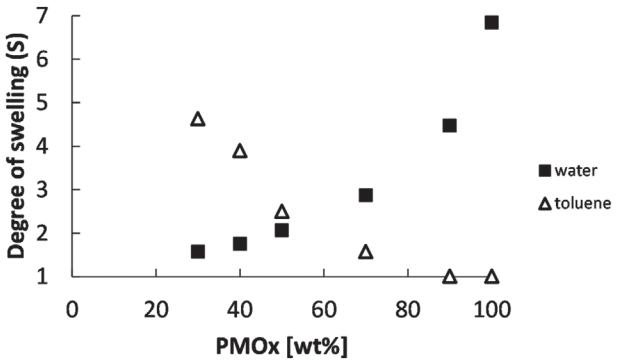

Figure 2. Degrees of swelling of PEhAc-*l*-PMOx conetworks in water (full squares) and toluene (empty triangles). The errors are less than 10% in all cases.

more than 70 wt% PMOx. This behavior was expected due to the amphiphilic character of the networks and is in accordance with the results of Sittko et al.[14a] Furthermore, Figure 1 seems to show that no matter how the polymers are connected, the solvent uptake and thus the structural change caused by this is only dependent on the mass fraction of the respective polymer phase. Whether this is truly the case is the objective of the following SAXS investigations.

Figure 3 shows the detected SAXS profiles of the conetworks in the dry state. First, a network consisting only of the hydrophilic PMOx was investigated. The SAXS curve does not show a correlation peak q^*. This means that no phase separation could be detected. This was expected, because the network consists of only one phase, as the end groups used for crosslinking are too small to form a detectable separated phase.

The addition of just 10 wt% hydrophobic PEhAc (PEhAc-*l*-PMOx(90)) causes a distinct correlation peak q^* at 0.095 Å^{-1} in the SAXS curve. This means that the presence of only 10 wt% PEhAc leads to a clearly distinguishable phase separation in the network. The structural correlations between the q^* value and the average long distance between two domains of one polymer phase were determined according to the calculation $d^* = 2\pi/q^*$.[27] The SAXS plots are depicted in Figure 3 and the d values are given in **Table 2**. According to this, the d value of an APCN with 90 wt% PMOx is 6.6 nm. Decreasing the hydrophilic component to 70 wt% PMOx leads to a strong correlation peak at 0.071 Å^{-1}, which corresponds to a d value of 9.2 nm. Further decreasing of the PMOx amount in the network to 50 and 30 wt% PMOx, respectively, leads to successively increasing d values of 10.8 and 12.6 nm.

This is expected, because the average long distance, d, is the addition of the sizes of the PMOx phase and the acrylate phase. While the PMOx phase is composed of defined polymeric segments with a narrow dispersity, $Đ$, the acrylate phase is composed of free radically polymerized segments with a broad $Đ$ value. The addition of both phases will eventually lead to an overall broad size distribution of d with increasing acrylate content.

These findings coincide with AFM images recorded by Sittko et al. for the same APCN system.[14a] They confirmed a homogeneous nanophase separation of the conetworks. The AFM images of the APCNs revealed that the thickness of the PMOx domain is nearly constant and independent of the networks composition, whereas the thickness of the PEhAc domains increases with increasing PEhAc content.

We calculated the domain size of each polymer phase in the APCN by fitting them numerically to the respective conetwork

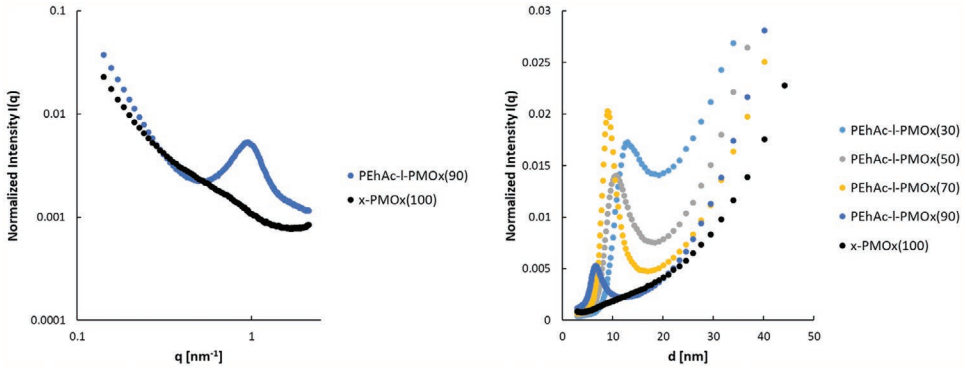

Figure 3. SAXS profiles obtained from dry PEhAc-*l*-PMOx conetworks with a PMOx content of 30–100 wt% (left: q-values, right: domain size $d = 2\pi/q$). Intensities were accumulated over 4 h and normalized to the overall counts of the respective measurement.

Table 2. Domain sizes in PEhAc-*l*-PMOx conetworks in the dry state.

APCN	d^*_{dry} [nm][a)]	d^*_{PMOx} [nm][b)]	d^*_{EhAc} [nm][b)]
PEhAc-*l*-PMOx(30)	12.6	5.2	7.4
PEhAc-*l*-PMOx(50)	10.8	5.2	5.6
PEhAc-*l*-PMOx(70)	9.2	5.1	4.1
PEhAc-*l*-PMOx(90)	6.8	4.5	2.3

[a)]Determined from the SAXS plots; [b)]Numerically fitted to meet the composition of the respective APCN presuming a cubic structure, ρ(PEhAc) = 0.903 g cm^{-3}, ρ(PMOx) = 1.14 g cm^{-3}.

composition. This was done presuming a cubic structure. The results are summarized in Table 2 and show that the calculated data support the AFM images by showing that the PMOx domains are of similar size in all APCNs.

Swelling of these structures will lead to different scenarios that are illustrated in **Figure 4**. We expected that the swelling should be dominated by the conetwork topology. The hydrophilic PMOx chains, which act as the crosslinkers, can only form domains by aggregation. These domains are covalently linked by the hydrophobic PEhAc, that is, the PMOx domains are always separated by a hydrophobic polymer chain. The PEhAc domains on the other hand are always connected. Figure 4 illustrates the different swelling scenarios that are presumed according to the network topology. Here, the structure formed by nanophase separation was taken from the AFM image of the APCN with 70 wt% PMOx. The PMOx domains in the PEhAc matrix are clearly visible. The AFM images of all other compositions show similar phase morphology with differently sized hydrophobic domains.[14a]

Swelling of the network in toluene (Figure 4, bottom right) would allow the whole PEhAc phase to swell, because it is fully

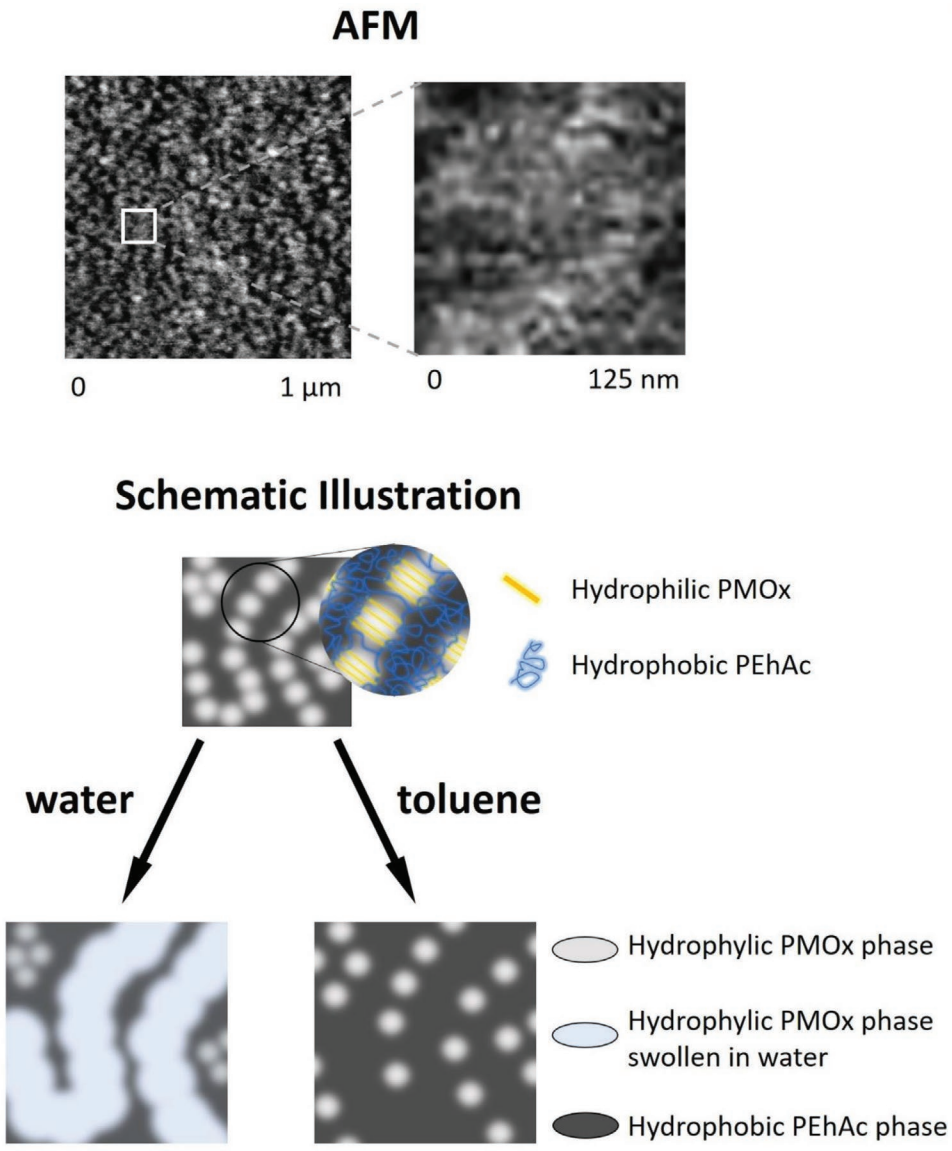

Figure 4. AFM image of the dry APCN PEhAc-*l*-PMOx(70) 1 × 1 µm (top) and schematic illustrations of the magnified image in dry (middle) and the swollen phases in water (bottom, left) and in toluene (bottom, right).

interconnected due to the network topology rather than the nanophase structure. The PMOx domains are then scattered and isolated in the swollen phase. Due to the broad molecular weight distribution of the acrylate phase, the well-ordered structures in the dry state might lose this order upon swelling. Swelling the same APCN in water, will afford the PMOx domains to swell and partially fuse to form larger domains (Figure 4, bottom left). Since the PMOx is not connected by network topology, there will always be non-swollen areas.

In order to investigate the swollen APCNs, they were placed into quartz glass capillaries that contained the respective solvent. These capillaries were then sealed at the ends by melting the glass.

First, the samples were analyzed in toluene filled capillaries after 24 h of swelling. Here, the swollen phase is always connected according to the conetwork topology. The rather isolated PMOx phase, which is not connected, has a high T_g (T_g = 80 °C) compared to PEhAc (T_g = –66 °C) and thus can hinder the swelling if it forms a continuous phase upon nanophase separation. As seen in **Figure 5**, in all cases the d^* values increase. However, the swelling causes different changes in the structural order indicated by less pronounced q^* correlation peaks. The APCN with a low acrylate content of 10 wt% and a degree of swelling of $S_{toluene}$ = 1.05 keeps the order and the only slightly increase of d^* from 6.6 to 7.2 nm supports this. The reason for the low degree of swelling of the most likely fully connected EhAc phase is the high T_g of the PMOx phase, which resists the expansion of first phase. Further increasing the acrylate content to 70 and 50 wt%, respectively, leads to stronger swelling in the non-polar solvent, which results in significant shifts of the d^* values from 12.6 to 18.4 nm for PEhAc-*l*-PMOx(30) and from 10.8 to 13.8 nm for PEhAc-*l*-PMOx(50). In both cases, the swollen networks show less pronounced correlation peaks, which indicate a loss of structural order compared to the respective dry APCNs. This is most likely due to continuous phases formed by PMOx, which keeps the overall structure due to the high T_g. APCNs with higher acrylate content also show an increased average long distance in the SAXS, but the signal is only a shoulder indicating that the order of the network is greatly disturbed. This might be due to the above mentioned structural change of the PMOx phases that are now embedded in an acrylate matrix with a broad molecular weight distribution. This would lead to greatly different local degrees of swelling and thus to a loss of the ordered structure (see Figure 4).

A different picture can be seen in cases of the water-swollen APCNs. Here, the high T_g PMOx phase swells and the low T_g acrylate phase will follow the structural changes caused by the different compositions. As seen in **Figure 6**, the SAXS plots are not comparable to those of the respective toluene-swollen APCNs. The sample with the lowest PMOx content of 30 wt% and a degree of swelling of S_{water} = 1.8 shows an unexpectedly great shift in the phase size, which indicates a significant change in order of the network, for example, due to the fusion of previously isolated domains (Figure 4, bottom, left). The SAXS plot of this water-swollen conetwork shows only a shoulder and thus a less ordered structure is indicated. Closer inspection of this plot (better seen in the respective Kratky plot, Figure 6) reveals a signal that can be attributed to a long distance of about 7 nm that remains in the swollen samples. This might be due to the fact that the swollen PMOx phase is not fully connected and thus isolated regions are not swollen. The long distance of d^* ≈7 nm was found for APCNs with 90 wt% PMOx, which suggests that these regions are PMOx enriched and probably caused by a partial phase separation of PMOx and PEhAc. The SAXS plot of the APCN with 50 wt% PMOx is even

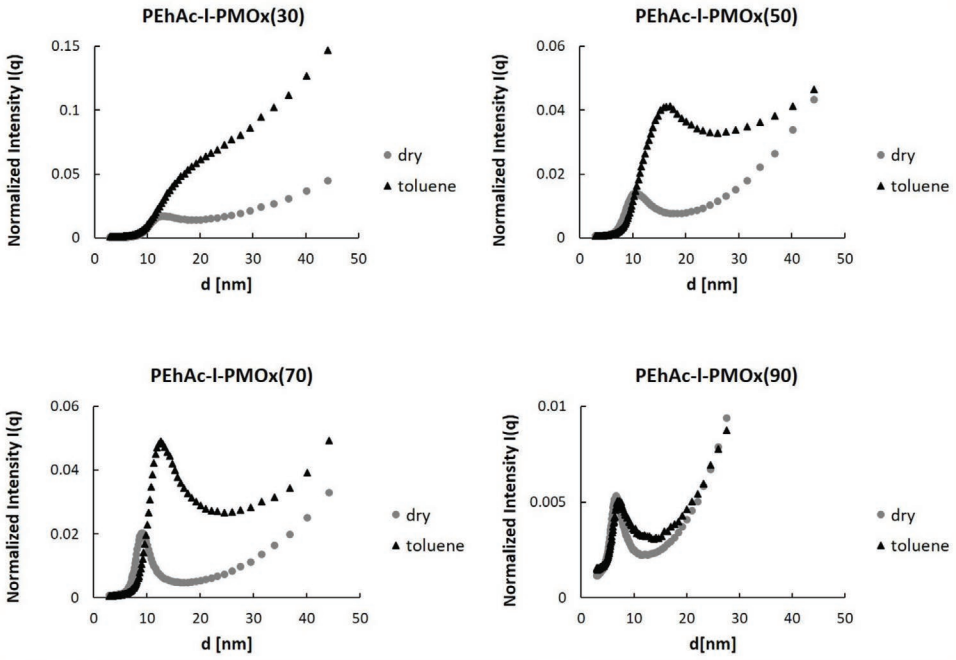

Figure 5. SAXS profiles obtained from PEhAc-*l*-PMOx conetworks with a PMOx content of 30–90 wt% that were swollen in toluene. Intensities were accumulated over 4 h and normalized to the overall counts of the respective measurement.

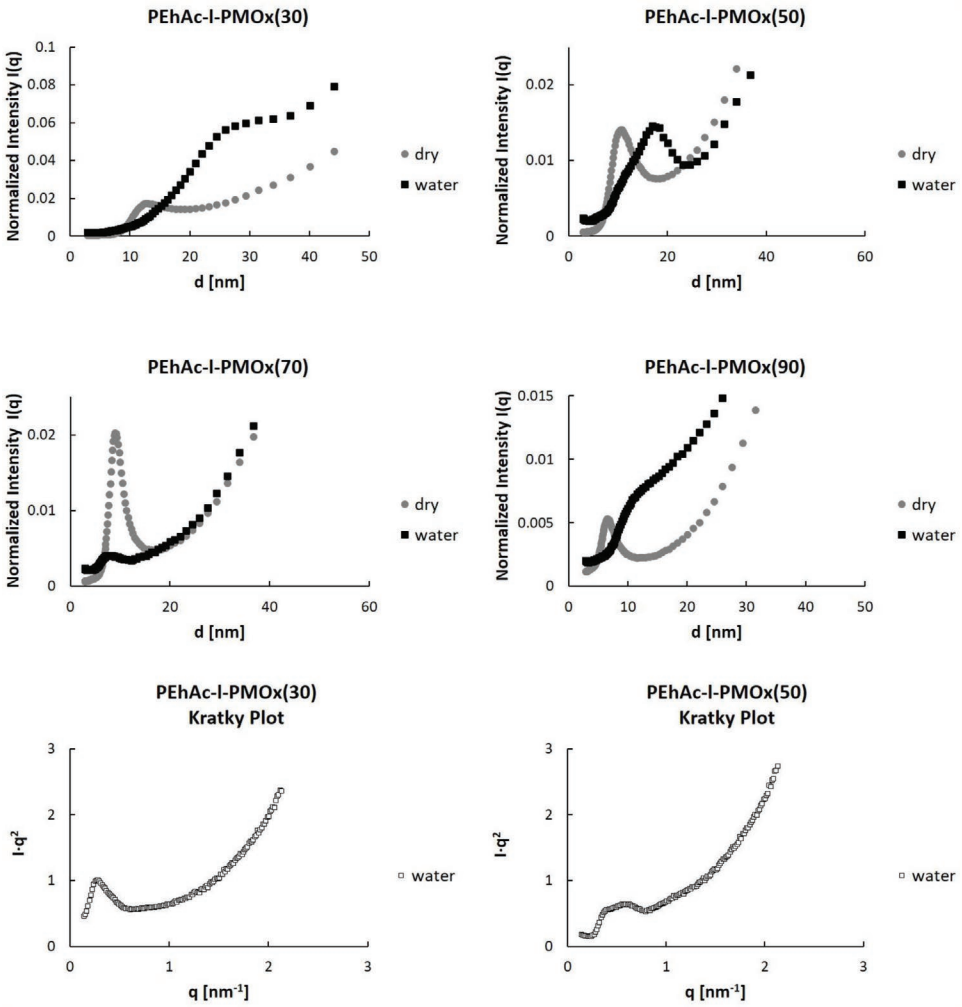

Figure 6. SAXS profiles obtained from PEhAc-*l*-PMOx conetworks with a PMOx content of 30–90 wt% that were swollen in water and Kratky plots of PEhAc-*l*-PMOx conetworks with a PMOx content of 30–50 wt%. Intensities were accumulated over 18 h and normalized to the overall counts of the respective measurement.

more complex showing a greatly shifted main peak that indicates swelling of the majority of the hydrophilic phases without losing order. However, this peak contains a shoulder that indicates structures with long distances found in the dry sample. This could be regions that are not reached by the solvent. Further, a minor signal can be distinguished at about 7 nm long distance that might be related to the above mentioned PMOx enriched separated phases. When swelling the APCN with 70 wt% PMOx in water, the SAXS plot shows no distinguishable signal that can be attributed to swelling of the phases indicating completely disordered conetwork. The only clear signal is that of the isolated non-swollen PMOx enriched phases at some 7 nm long distance. The swelling of the APCN with 90% PMOx shows a similar picture with a somewhat better distinguishable shoulder of the swollen domains.

The domain size change upon swelling was calculated by presuming that the phases swell selectively in the respective solvent. Thus, all the solvent taken up upon swelling (degree of swelling see Figure 2) increases the volume of the domains (dry domain size calculated in Table 2). It was further assumed for the sake of this calculation that the swelling occurs without changing the structure. **Figure 7** depicts the calculated domain sizes and the domain sizes measured with SAXS. In case of the swelling in toluene, the measured domain sizes nicely correlate with the calculated ones. The data obtained from the water-swollen APCNs are also following the same trend, but the measured domain sizes are always larger than the calculated ones. This might be explainable by a change in order of the network upon swelling in water, which would lead to larger domains caused by swelling induced structural changes, for example, the fusion of PMOx phase to larger structures (see Figure 4, bottom left). Another explanation could be that the water does not reach all regions in the networks as indicated by the additional smaller domains in the SAXS plot. This will then lead to higher swelling of the domains that are reached by the solvent.

Altogether, the different structural changes upon swelling of the APCNs in water and toluene indicated in the SAXS plots can be explained by the topology of the conetwork according to the model shown in Figure 4.

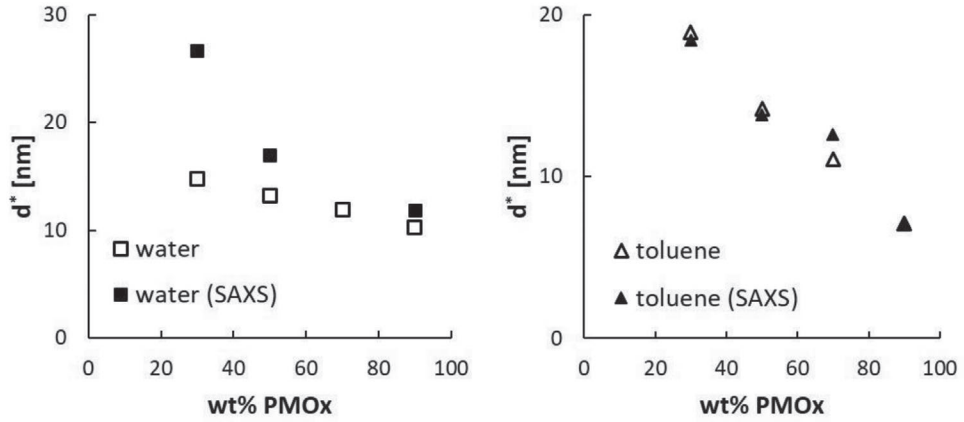

Figure 7. Domain size of PEhAc-*l*-PMOx conetworks calculated from the degree of swelling in water (empty squares) and toluene (empty triangles) compared to the corresponding d^* values of the SAXS measurements (full squares and triangles).

3. Conclusions

The SAXS measurements presented here on APCNs swollen in orthogonal solvents revealed that structural change upon swelling is strongly dependent on the topology of the APCN. The investigated APCNs are prepared by the most often applied approach of crosslinking a free radically polymerized monomer with a narrowly distributed macromolecular crosslinker. The nanophase separation shown by AFM or TEM and the swelling data of these APCNs suggest a homogeneous swelling of each individual polymer phase with a respective selective solvent over a broad range of compositions. SAXS data revealed that this is not true for both phases, but the crosslinker phase is more isolated than suggested by AFM and TEM images and the selective solvent is not fully swelling this phase excluding isolated non-swollen regions. This finding is of importance for the applications of APCNs particularly in fields of drug delivery. Further, the present study shows that it might be useful to investigate APCNs more thoroughly with scattering methods to better reveal their true swelling behavior.

4. Experimental Section

Instruments: ^{1}H NMR spectra were recorded in $CDCl_3$ using a Nanobay AVANCE-III HD-400 spectrometer with a 5 mm BBFOsmart probe from Bruker BioSpin GmbH operating at 400 MHz and a DD2-500 spectrometer with 5 mm triple resonance H(C,X) probe from Agilent Technologies operating at 500 MHz.

The microwave-assisted polymerizations were carried out in CEM Discover synthesis microwaves. The reaction temperature was constantly monitored using a vertically focused IR temperature sensor.

Infrared spectroscopy analysis was carried out using a spectrometer Alpha P (Bruker) in attenuated total reflection (ATR). The spectra of the networks were recorded with a resolution of 4 cm^{-1} and 24 scans per minute with a wave length range from 400 to 4000 cm^{-1} and processed with OPUS software.

X-ray scattering patterns were recorded using a Bruker NANOSTAR composed of a micro focus X-ray source (IμS, Incoatec GmbH) with a Cu-anode and integrated Montel Optic and a VANTEC-2000 detector. The distance of the sample and the detector was 107 cm and a calibration was performed with Ag-behenate standard. The measurements were carried out under vacuum. For that purpose the swollen networks were filled in quartz glass capillaries, which were sealed on both ends. The measurements of the dry networks and the APCNs swollen in toluene were conducted for 4 h and the measurements of the water-swollen APCNs were carried out for 18 h. The X-ray patterns were azimuthally integrated to the scattered intensities as a function of the magnitude of the scattering vector $q = 4\pi\sin(\theta)/\lambda$ (with θ = diffraction angle, $\lambda = 1.5406$ Å).

AFM images were recorded with a Veeco Dimension Icon scanning probe microscope (Veeco Instruments) equipped with a Nanoscope V Controller and an AVH-1000 Workstation. All measurements were conducted in tapping mode using commercial tapping mode etched silicon probe cantilevers of various frequencies from 300 to 400 kHz. Phase images were recorded at 5% below the fundamental resonance frequency of the cantilever, with a typical scan speed of 1 Hz and a resolution of 512 samples per line for a 1 μm scan size.

Materials: All purifications and reactions were performed under argon atmosphere. Chloroform (Fisher Chemical) was distilled from activated aluminum oxide (Merck) under reduced pressure. It was stored under argon atmosphere over molecular sieves (4 Å). *trans*-1,4-Dibromo-2-butene (DBB) was purchased from Sigma-Aldrich and recrystallized twice from *n*-heptane (VWR). 2-Methyl-2-oxazoline (MOx) was purchased from Acros, distilled over CaH_2 (Acros), and stored under argon atmosphere at −20 °C. *N*-[3-(Dimethylamino)-propyl]-methacrylamide (DMAP-MAA) and EhAc were purchased from Sigma-Aldrich. They were distilled for purification, stored under argon atmosphere at −20 °C, and used within two weeks. The photoinitiator Irgacure 651 was kindly provided by Ciba Specialty Chemicals (now part of BASF, Basel, Switzerland).

All other chemicals were purchased in analytical grade and used without further purification.

Synthesis of Poly(2-methyl-2-oxazoline) with DMAP-MAA End Groups: The telechelic PMOxs was prepared according to literature.[14a] The cationic ring opening polymerization of MOx (5 mL, 59 mmol, 30 eq.) with DBB (421 mg, 1.97 mmol, 1 eq.) as initiator was carried out in 20 mL of dry chloroform under argon atmosphere in an industrial microwave reactor at 100 °C for 4 h. The living ends of the polymers were terminated with DMAP-MAA in a 12-fold molar excess at 45 °C for 48 h. The raw polymeric product was purified by precipitating the polymers in ice-cold diethyl ether and then dialyzed against methanol using benzoylated cellulose membranes (1000 MWCO). The methanol was removed under reduced pressure and purified polymers with two acrylamide end groups were obtained in a yield of 80%.

^{1}H NMR (400 MHz, $CDCl_3$-*d*) $\delta = 1.95$ (br. s., 6 H, $CH_3{-}CCH_2$) 1.99–2.34 (m, 105 H, $CH_3{-}CO{-}N$) 2.42 (br. s., 4 H, $NH{-}CH_2{-}CH_2{-}CH_2$) 3.25 (br. s., 12 H, $N(CH_3)_2$) 3.32–3.85 (br. s., 139 H, $N{-}(CH_2)_2$; $NH{-}CH_2{-}CH_2{-}CH_2$) 3.94 (br. s., 4 H, $CH_2{-}CH$) 5.35 (br. s., 2 H, CCH_2) 5.56 (br. s., 1 H, $CH_2{-}CH$) 5.84 (br. s., 1 H, CCH_2) ppm.

Synthesis of Amphiphilic Polymer Conetworks: The APCNs were synthesized as described in ref. [14a]. The telechelic PMOx was dissolved in 1-methoxy-2-propanol (1M2P). EhAc was added in different amounts and the reactants were mixed until completely diluted. The used amount of each component is given in Table 1. After adding 2 mg of Irgacure 651, the solution mixture was placed between two microscope slides, which were covered with adhesive poly(propylene)-tape (PP; Tesafilm). The polymerization was carried out under UV flash light (Heraeus Kulzer, Typ Heraflash, Germany, $\lambda = 340$ nm) for 3×180 s on each side. After polymerization the networks were removed from the glass slides and washed in chloroform for 24 h. The thickness of the resulting clear films was about 50 µm. Then the gel content was determined by the mass loss after washing and the composition was determined using FTIR-ATR measurements according to Sittko et al.[14a] The conetworks did not significantly change their composition according to the latter measurement (see Table S1, Supporting Information).

Determination of the Swelling Behavior: The swelling behavior of the PEhAc-*l*-PMOx films was determined gravimetrically. To this end, 100 mg of a sample was swollen in water or toluene, respectively, for 24 h and weighed. The degree of swelling was calculated from the quotient of the weights of the swollen and the dry film.

Supporting Information

Supporting Information is available from the Wiley Online Library or from the author.

Acknowledgements

The authors would like to thank Volker Brandt for performing AFM measurements, Dr. Wolf Hiller and his team from the Department of Chemistry for recording the NMR spectra at the TU Dortmund, and the glassblowing facility of the TU Dortmund for sealing the quartz capillaries. All polymers were synthesized using CEM Discover microwaves, which were kindly provided by CEM for undergraduate student education.

Open access funding enabled and organized by Projekt DEAL.

Conflict of Interest

The authors declare no conflict of interest.

Keywords

amphiphilic polymer conetworks, poly(2-ethylhexyl acrylate), poly(2-oxazoline), small-angle X-ray scattering

Received: September 2, 2020
Revised: October 12, 2020
Published online: November 23, 2020

[1] a) G. Erdodi, J. P. Kennedy, *Prog. Polym. Sci.* **2006**, *31*, 1; b) C. S. Patrickios, in *Amphiphilic Polymer Co-Networks: Synthesis, Properties, Modelling and Applications*, (Ed: C. S. Patrickios), The Royal Society of Chemistry, London **2020**, pp. 1–14.
[2] Z. Mutlu, S. S. Es-haghi, M. Cakmak, *Adv. Healthcare Mater.* **2019**, *8*, 1801390.
[3] J. P. Kennedy, G. Fenyvesi, S. Na, B. Keszler, K. S. Rosenthal, *Des. Monomers Polym.* **2000**, *3*, 113.
[4] S. He, M. J. Yaszemski, A. W. Yasko, P. S. Engel, A. G. Mikos, *Biomaterials* **2000**, *21*, 2389.
[5] J. C. Tiller, C. Sprich, L. Hartmann, *J. Controlled Release* **2005**, *103*, 355.
[6] a) M. Hanko, N. Bruns, J. C. Tiller, J. Heinze, *Anal. Bioanal. Chem.* **2006**, *386*, 1273; b) M. Hanko, N. Bruns, S. Rentmeister, J. C. Tiller, J. Heinze, *Anal. Chem.* **2006**, *78*, 6376.
[7] a) G. Kali, T. K. Georgiou, B. Iván, C. S. Patrickios, E. Loizou, Y. Thomann, J. C. Tiller, *Langmuir* **2007**, *23*, 10746; b) G. Kali, S. Vavra, K. László, B. Iván, *Macromolecules* **2013**, *46*, 5337; c) J. Bünsow, M. Mänz, P. Vana, D. Johannsmann, *Macromol. Chem. Phys.* **2010**, *211*, 761; d) S. Ulrich, A. Osypova, G. Panzarasa, R. M. Rossi, N. Bruns, L. F. Boesel, *Macromol. Rapid Commun.* **2019**, *40*, 1900360; e) B. Iván, M. Haraszti, G. Erdődi, J. Scherble, R. Thomann, R. Mülhaupt, *Macromol. Symp.* **2005**, *227*, 265; f) M. R. Simmons, E. N. Yamasaki, C. S. Patrickios, *Macromolecules* **2000**, *33*, 3176; g) S. Pásztor, B. Iván, G. Kali, *J. Polym. Sci., Part A: Polym. Chem.* **2017**, *55*, 1818; h) J. Feldthusen, B. Iván, A. H. E. Müller, J. Kops, *Macromol. Symp.* **1996**, *107*, 189; i) M. Haraszti, E. Tóth, B. Iván, *Chem. Mater.* **2006**, *18*, 4952.
[8] J. Tobis, Y. Thomann, J. C. Tiller, *Polymer* **2010**, *51*, 35.
[9] a) J. Tobis, L. Boch, Y. Thomann, J. C. Tiller, *J. Membr. Sci.* **2011**, *372*, 219; b) J. Tobis, J. C. Tiller, *Biotechnol. Lett.* **2014**, *36*, 1661.
[10] K. R. McLeod, G. N. Tew, *Macromolecules* **2017**, *50*, 8042.
[11] C. Mugemana, P. Grysan, R. Dieden, D. Ruch, N. Bruns, P. Dubois, *Macromol. Chem. Phys.* **2020**, *221*, 1900432.
[12] a) G. Savin, N. Bruns, Y. Thomann, J. C. Tiller, *Macromolecules* **2005**, *38*, 7536; b) I. Schoenfeld, S. Dech, B. Ryabenky, B. Daniel, B. Glowacki, R. Ladisch, J. C. Tiller, *Biotechnol. Bioeng.* **2013**, *110*, 2333; c) S. Dech, T. Cramer, R. Ladisch, N. Bruns, J. C. Tiller, *Biomacromolecules* **2011**, *12*, 1594; d) N. Bruns, J. C. Tiller, *Nano Lett.* **2005**, *5*, 45.
[13] a) N. Bruns, W. Bannwarth, J. C. Tiller, *Biotechnol. Bioeng.* **2008**, *101*, 19; b) N. Bruns, J. C. Tiller, *Macromolecules* **2006**, *39*, 4386.
[14] a) I. Sittko, K. Kremser, M. Roth, S. Kuehne, S. Stuhr, J. C. Tiller, *Polymer* **2015**, *64*, 122; b) S. Dech, V. Wruk, C. P. Fik, J. C. Tiller, *Polymer* **2012**, *53*, 701.
[15] a) C. Fodor, G. Kali, R. Thomann, Y. Thomann, B. Ivan, R. Mulhaupt, *RSC Adv.* **2017**, *7*, 6827; b) C. Fodor, T. Stumphauser, R. Thomann, Y. Thomann, B. Ivan, *Polym. Chem.* **2016**, *7*, 5375.
[16] a) D. Kafouris, E. Themistou, C. S. Patrickios, *Chem. Mater.* **2006**, *18*, 85; b) T. C. Krasia, C. S. Patrickios, *Macromolecules* **2006**, *39*, 2467.
[17] a) C. Krumm, S. Konieczny, G. J. Dropalla, M. Milbradt, J. C. Tiller, *Macromolecules* **2013**, *46*, 3234; b) J. Cui, M. A. Lackey, G. N. Tew, A. J. Crosby, *Macromolecules* **2012**, *45*, 6104; c) J. Cui, M. A. Lackey, A. E. Madkour, E. M. Saffer, D. M. Griffin, S. R. Bhatia, A. J. Crosby, G. N. Tew, *Biomacromolecules* **2012**, *13*, 584; d) C. N. Walker, K. C. Bryson, R. C. Hayward, G. N. Tew, *ACS Nano* **2014**, *8*, 12376.
[18] a) N. Bruns, J. Scherble, L. Hartmann, R. Thomann, B. Iván, R. Mülhaupt, J. C. Tiller, *Macromolecules* **2005**, *38*, 2431; b) E. J. Kepola, E. Loizou, C. S. Patrickios, E. Leontidis, C. Voutouri, T. Stylianopoulos, R. Schweins, M. Gradzielski, C. Krumm, J. C. Tiller, M. Kushnir, C. Wesdemiotis, *ACS Macro Lett.* **2015**, *4*, 1163; c) D. E. Apostolides, C. S. Patrickios, T. Sakai, M. Guerre, G. Lopez, B. Améduri, V. Ladmiral, M. Simon, M. Gradzielski, D. Clemens, C. Krumm, J. C. Tiller, B. Ernould, J.-F. Gohy, *Macromolecules* **2018**, *51*, 2476.
[19] J. Scherble, R. Thomann, B. Iván, R. Mülhaupt, *J. Polym. Sci., Part B: Polym. Phys.* **2001**, *39*, 1429.
[20] a) A. Domján, G. Erdödi, M. Wilhelm, M. Neidhöfer, K. Landfester, B. Iván, H. W. Spiess, *Macromolecules* **2003**, *36*, 9107; b) C. N. Tironi, R. Graf, I. Lieberwirth, M. Klapper, K. Müllen, *ACS Macro Lett.* **2015**, *4*, 1302; c) A. Domján, C. Fodor, S. Kovács, T. Marek, B. Iván, K. Süvegh, *Macromolecules* **2012**, *45*, 7557.
[21] E. N. Kitiri, C. K. Varnava, C. S. Patrickios, C. Voutouri, T. Stylianopoulos, M. Gradzielski, I. Hoffmann, *J. Polym. Sci., Part A: Polym. Chem.* **2018**, *56*, 2161.

[22] a) D. Zeng, A. Ribbe, R. C. Hayward, *Macromolecules* **2017**, *50*, 4668; b) S. Ulrich, A. Sadeghpour, R. M. Rossi, N. Bruns, L. F. Boesel, *Macromolecules* **2018**, *51*, 5267.
[23] B. Y. Shekunov, P. Taylor, J. G. Grossmann, *J. Cryst. Growth* **1999**, *198-199*, 1335.
[24] a) X. Zhang, K. Kyriakos, M. Rikkou-Kalourkoti, E. N. Kitiri, C. S. Patrickios, C. M. Papadakis, *Colloid Polym. Sci.* **2016**, *294*, 1027; b) M. Rikkou-Kalourkoti, E. N. Kitiri, C. S. Patrickios, E. Leontidis, M. Constantinou, G. Constantinides, X. Zhang, C. M. Papadakis, *Macromolecules* **2016**, *49*, 1731.
[25] T. Hiroi, S. Kondo, T. Sakai, E. P. Gilbert, Y.-S. Han, T.-H. Kim, M. Shibayama, *Macromolecules* **2016**, *49*, 4940.
[26] D. Park, B. Keszler, V. Galiatsatos, J. P. Kennedy, *J. Appl. Polym. Sci.* **1997**, *66*, 901.
[27] B. Iván, K. Almdal, K. Mortensen, I. Johannsen, J. Kops, *Macromolecules* **2001**, *34*, 1579.